

BEHAVIOR OF CONCRETE FILLED STAINLESS STEEL TUBULAR COLUMN UNDER AXIAL LOADS

Lieutenant Colonel Muhammad Sanaullah⁽¹⁾, Jesika Rahman⁽²⁾, Ibriju Ibrahim⁽³⁾
and Major Md. Soebur Rahman⁽⁴⁾

1. General Staff Officer-Grade-1 (Research), Military Institute of Science and Technology
Mirpur Cantonment, Dhaka-1216, Bangladesh
E-mail: mssanaul35@gmail.com
2. Lecturer, CE Department, Military Institute of Science and Technology
Mirpur Cantonment, Dhaka-1216, Bangladesh E-mail: jesikarahman547 @ce.mist.ac.bd
3. Research Assistant, CE Department, Military Institute of Science and Technology
Mirpur Cantonment, Dhaka-1216, Bangladesh E-mail: Ibrijuibrahim @gmail.com
4. Instructor Class-“A”, CE Department, Military Institute of Science and Technology
E-mail: soeburrahman@gmail.com

ABSTRACT

Concrete filled stainless steel tube (CFSST) is a composite structure that comprises both the structural steel and core concrete. A CFSST column has gained prominence from structural engineers all over the world as it provides sufficient strength and durability to withstand compressive loads. Use of stainless steel in place of mild steel provides the desired fire and corrosion resistance, as well as aesthetics otherwise a concrete filled steel tube (CFST) would be unable to. Due to its superior fire and corrosion resistance, stainless steels are used as a structural member in various constructions. This paper presents a detailed experimental and numerical study on the compressive behavior of concrete filled stainless steel tubular columns subjected to concentric loading. Hollow stainless tubes are also studied for comparison. Numerical models are developed using general purpose finite element (FE) software ABAQUS and have been validated using the experimental data of the present study as well as recently published test results. The FE models predict the experimental load-deformation behavior, ultimate strength and failure modes with good accuracy. Once the FE model is validated, the numerical results are compared with the existing conventional carbon steel design code/guidelines and developed a prediction formula for CFSST columns.

Key words: Stainless Steel, Concrete Filled Tube, Finite Element Modeling, Composite Structure

1.0 INTRODUCTION

The use of composite structures dates back to the eighteenth century in the United States¹. A composite structural member comprising both structural steel and core concrete has gained tremendous popularity worldwide due to increased strength and larger usable space. The Concrete Filled Stainless Steel Tube (CFSST) is a composite column where the steel tube, having a rectangular or circular cross-section, is infilled with normal or high strength concrete. The local inward buckling being reduced, the concrete fill inside adds confinement and compressive strength to the column². It is because of the composite action of

steel and concrete that the CFSST column inhibits excellent seismic and fire resistance^{3,4}. Moreover, the steel section behaves as the formwork and reduces the cost of labor in the construction phase.

Till date, many researchers have studied the performance of concrete filled carbon steel tubular (CFST) columns^{5,6,7} whereas research on CFSST columns is still in its early stages. Schneider and Huang et al. concluded that circular steel sections in a CFST provide greater post-yield axial ductility than other sections, namely square and rectangular^{8,9}. The applicability of various codes to determine the strength of CFST columns has been reported

by researchers¹⁰. Previously, moment-curvature response of square CFSST columns was analysed and reported¹¹. Researchers also reviewed the performance of CFSST in columns and joints as well as in bridges¹². The excellent potential of stainless steels in bridge construction has been investigated by researchers in the past¹³. Numerical analysis is one of the most popular techniques to study and predict the behavior of CFSST sections. Number of studies in the past is done on square CFSST stub columns and thin-walled stiffened stub columns both numerically and experimentally^{14,15,16}. However, no sufficient practical data yet exists to regulate a design guideline in order to make a CFSST compression member suitable for structural purposes. Hence, the paramount objective of the study is to gauge the behavior of CFSST columns under concentric axial loads by evaluating the results from property variations like concrete compressive strength and geometry of the steel sections. Upon the succession of which, it will be possible to select a reliable design guideline that allows the use of CFSST columns in wider implementations.

In this study, a total of ten CFSST short columns were tested to investigate their performance under compressive axial load. Five hollow stainless steel tubes are also included for comparison. Their performance due to changes in concrete compressive strength and steel section geometry were evaluated in terms of several tests carried out as described in the sections below. A nonlinear FE model was developed to simulate the compressive loading conditions on the column specimens. The results obtained from the model as well as that from a published literature were verified against the experimental results. In the final outset, two of the extensively used design codes, AISC and Eurocode 4 (EC4), were selected to predict the CFSST column strength which was then compared with the strength obtained experimentally and numerically.

2.0 EXPERIMENTAL PROGRAM

An experimental investigation was conducted to assess the compressive response, failure mode and load carrying capacity of CFSST columns. The test specimens were divided into five groups. Three types of cross-sections were included in the test series namely square, rectangular and circular hollow sections. For the comparison of performances, three

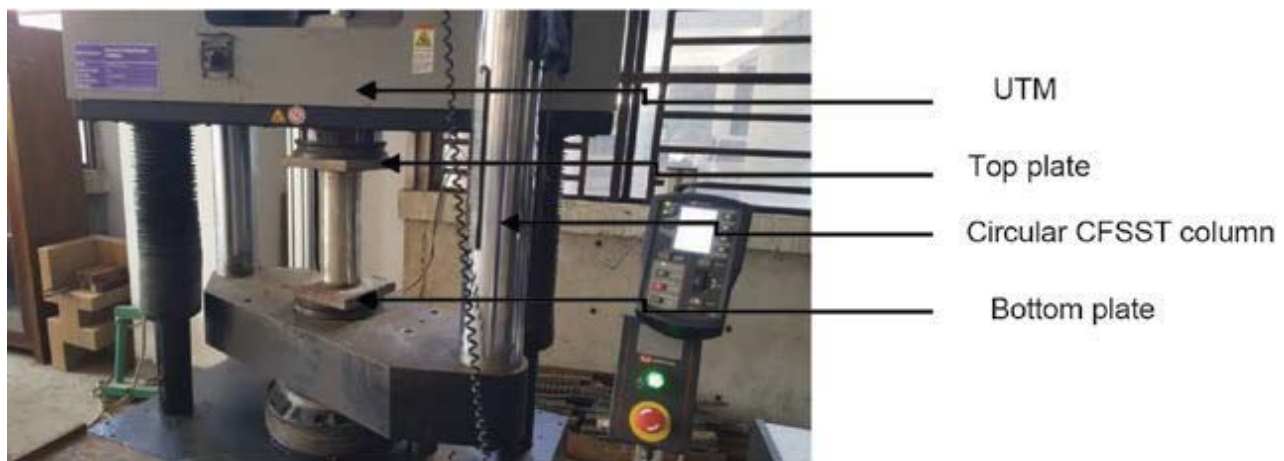
short column tests were carried out for each sections – two concrete filled specimens with concrete strengths of 30 MPa and 40 MPa and one hollow stainless tube.

2.1 Test specimen

Hollow stainless steel tubes were cold-formed sections cut in accordance with the required dimensions. Materials, available commercially, were used in the production of the concrete along with normal mixing and curing techniques. Stainless steel sections of Grade 203 was used in this study. Coupon test for the tensile properties of the stainless steel and cylinder test for the compressive strength of the concrete were carried out to monitor the strength of the constituent materials. Table 1 represents the dimensions of the specimens and material properties of concrete and stainless steel, where D is the depth of the square and rectangular sections and diameter for the circular sections, respectively. B , t and h represent the width, thickness of the plate section and height of the specimens respectively. E_c and E_s are the modulus of elasticity of concrete and stainless steel, f'_c is the compressive strength and ν is the Poisson's ratio of the concrete, $\sigma_{0.2}$ and σ_u are the 0.2% proof stress and ultimate tensile strength respectively and n is strain hardening exponent of the stainless steel section.

Table 1. Measured specimen dimension and material properties

Group Name	Specimens Designation	D X t X h (mm)	B (mm)	f'_c (MPa)	E_c (MPa)	$\sigma_{0.2}$ (MPa)	E0 (GPa)	n
G1	S1H	63.5 X 1.5 X 190.5	63.5	-	-	470	198	3.5
	S1C30			30	25743	470	198	3.5
	S1C40			40	29725	470	198	3.5
G2	S2H	76.2 X 1.5 X 228.6	50.8	-	-	470	198	3.5
	S2C30			30	25743	470	198	3.5
	S2C40			40	29725	470	198	3.5
G3	S3H	76.2 X 1.5 X 228.6	76.2	-	-	470	198	3.5
	S3C30			30	25743	470	198	3.5
	S3C40			40	29725	470	198	3.5
G4	S4H	101.6 X 1.5 X 304.8	50.8	-	-	470	198	3.5
	S430			30	25743	470	198	3.5
	S4C40			40	29725	470	198	3.5
G5	S5H	101.6 X 1.5 X 304.8	-	-	-	470	198	3.5
	S5C30			30	25743	470	198	3.5
	S5C40			40	29725	470	198	3.5

**Fig 1.** Experimental Set-up of CFSST Column

3.0 FINITE ELEMENT MODELLING

The general-purpose finite element program ABAQUS version 6.14 was used to build a nonlinear 3D FE model to investigate the behavior and strength of CFSST columns comprising the aforementioned variety in geometric and material properties. The stainless steel tube was modeled using four-node shell elements (S4R) and the concrete was modeled using 8 node brick elements (C3D8R). Surface-based interaction with a contact pressure model in the normal direction and a Coulomb friction model in the tangential directions was used to simulate contact between steel and core concrete. Although

there exists a cover of chemically stable chromium oxide for corrosion prevention of the stainless tube, the column's behavior is not sensitive to the selection of friction coefficient between steel and concrete. A coefficient of friction between the stainless tube and core concrete was therefore taken as 0.25 for the current study. The Poisson's ratio of steel and concrete were considered as 0.3 and 0.2, respectively. The damage plasticity model available in the ABAQUS package was used to model the concrete behavior. The modeling technique proposed in the previous study was used to model the concrete and stainless steel¹⁶. The technique proposed by another study was used to simulate the circular CFSST columns.

FE model of CFSST test specimens was developed. The load-deflection, as well as failure behavior obtained from the numerical simulation, were compared with that of the experimental results. All the column samples were designed to examine the behavior for concentric axial loading. A contrast between the experimental and numerical ultimate capacities of the samples are also presented in the following sections.

4.0 VALIDATION OF THE FINITE ELEMENT MODEL

4.1 Current Experimental and Numerical Investigation

FE model of CFSST test specimens was developed. The load-deflection, as well as failure behavior obtained from the numerical simulation, were compared with that of the experimental results. All the column samples were designed to examine the behavior for concentric axial loading. A contrast between the experimental and numerical ultimate capacities of the samples are also presented in the following sections.

4.1.1 Load-Deflection Behaviour

The maximum axial compressive load and corresponding strain, as determined from the numerical model are compared with that of the experimental data. The load-deflection behavior of the five groups of CFSST columns tested are illustrated in Figure 2 which shows that the FE simulation can predict the experimental results with good precision. From Table 2 it is seen that the circular sections exhibit greater capacity both experimentally and numerically. Also, the hollow sections in each group shows weaker strength compared to their counterparts. However, the peak load in G1 samples are found to vary by about 42% and 9% for the hollow and concrete filled sections respectively. The ratio of the experimental to numerical capacities, P_{exp}/P_{num} ranges from 0.93 to 1.11 and corresponding coefficient of variation (COV) of 0.06 which validates the numerical simulation further. Again, the ratio of the numerical to experimental average axial strain at peak load, $\epsilon_{num}/\epsilon_{exp}$, ranges from 0.940 to 1.07 and the corresponding COV of 0.09 is observed. Therefore, it is obvious that the FE model developed in this study is capable of predicting the ultimate capacity and corresponding peak strain of CFSST columns with very good accuracy.

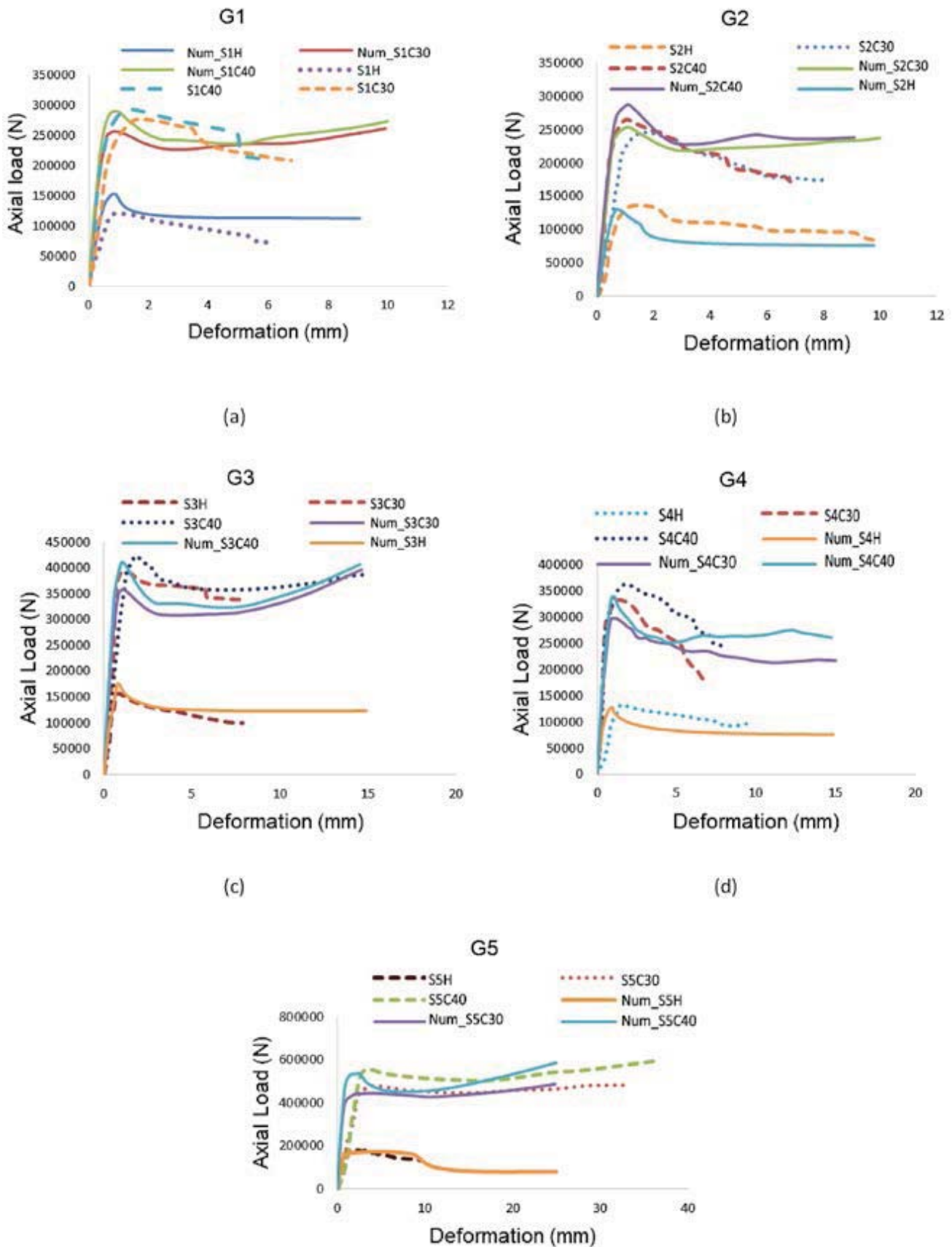


Fig 2. Experimental and Numerical Behaviour of CFSST Column Specimens

Table 2. Comparison between experimental and numerical analysis CFSST strengths

Group Name	Specimens Designation	Peak axial load		P_{exp} / P_{num}	Axial Strain at Peak Load		
		P_{exp} (kN)	P_{num} (kN)		Experimental $\epsilon_{exp}(\mu\epsilon)$	Numerical $\epsilon_{num}(\mu\epsilon)$	$\epsilon_{exp} / \epsilon_{num}$
G1	S1H	137	126	1.09	5578	5526	1.01
	S1C30	276	257	1.07	5521	5517	1.00
	S1C40	293	289	1.01	6210	5935	1.05
G2	S2H	133	132	1.01	4181	4097	1.02
	S2C30	242	254	0.95	4824	4729	1.02
	S2C40	266	287	0.93	4773	4767	1.00
G3	S3H	158	171	0.93	4573	4486	1.02
	S3C30	391	358	1.09	4736	4809	0.98
	S3C40	413	411	1.01	4956	4989	0.99
G4	S4H	132	121	1.09	3345	3451	0.97
	S4C30	330	298	1.11	3465	3403	1.02
	S4C40	359	340	1.06	3561	3501	1.02
G5	S5H	177	173	1.02	11429	12802	0.89
	S5C30	478	444	1.08	12685	13201	0.96
	S5C40	552	535	1.03	12278	9250	1.33
			Mean	1.03		Mean	1.02
			COV	0.06		COV	0.09

4.1.2 Failure Modes

Comparison between the failure modes obtained from the FE analysis and that of the experimental observation from the current study were made. Photographed images of failure modes of the specimens under concentric axial load were used to serve the purpose. It was observed that the failure pattern varied mostly due to changes in cross-section and slightly due to a change in concrete strength. The main failure was at the corner due to bulging out of concrete in rectangular columns filled with

concrete. However, for circular sections, the main failure was due to buckling. Concrete crushing prevailed the yielding of the stainless steel during the experiment. A good resemblance in failure pattern was found in the developed FE model for the same loads applied. The typical failure behavior under the axial compressive load are highlighted in Figure 3. The failure pattern predicted by the model presented in the study resembled quite well to that of the observed experimentally adding more to the proof of accuracy of the numerical model.



(a) Square CFSST Column



(b) Circular CFSST Column

Fig 3. Failure modes observed from experimental results

Table 3. Geometrical and material properties of the specimens¹⁶

Sl No.	Specimens Designation	BxtxL (mm)	Properties of Concrete			Properties of Stainless Steel		
			E _c (MPa)	f' _c (MPa)	v	E ₀ (MPa)	σ _{0.2} (MPa)	n
1	S20-50x3-A	51x2.85x150	21795	21.5	0.2	207900	440	8.2
2	S20-100x5-A	101x5.05x300	21795	21.5	0.2	202100	435	7
3	S30-100x3-A	101x2.85x300	27765	34.9	0.2	195700	358	8.3
4	S30-150x3A	152x2.85x450	27765	34.9	0.2	192600	268	6.8
5	SHS1C40	150.5x5.83x450	32084	46.6	0.2	194000	497	3
6	SHS-5-C60	100x4.9x300	34216	53	0.2	180000	458	3.7

Table 4: Comparison between the experimental capacity of specimens¹⁶ and numerical capacity (current study)

Sl No.	Specimens Designation	f' _c (MPa)	Peak axial load			Axial Strain at Peak Load		
			P _{exp} (kN)	P _{num} (kN)	P _{exp} /P _{num}	ε _{exp} (με)	ε _{num} (με)	ε _{exp} /ε _{num}
1	S20-50x3-A	21.5	363	378	0.96	10000	10300	0.97
2	S20-100x5-A	21.5	1360	1290	1.05	9800	9500	1.02
3	S30-100x3-A	34.9	764	791	1.06	4630	4900	1.02
4	S30-150x3-A	34.9	1178	1203	0.98	3700	4000	0.93
5	SHS1C40	46.6	2745	3029	0.91	10000	10000	1.00
6	SHS-5-C60	53	1565	1499	1.04	7700	8300	0.93
				Mean	0.99			0.98
				COV	0.06			0.04

Figure 4 represents the numerical capacities predicted by the model as well as experimental capacities of the published study¹⁶ and the numerical capacity as predicted by the model generated in this study. Close agreement in the results is observed between the published and the current models, respectively.

5.0 COMPARISON BETWEEN CODE PREDICTIONS AND NUMERICAL RESULTS

5.1 Existing Design Codes of Practice

The axial strengths obtained from the test results as represented in this paper are compared with that of the codes practiced internationally for the design of steel-concrete composite members. Two such codes, the American Specification AISC-2015¹⁹, the Eurocode 4 (EC4)²⁰ are nominated for the subsequent study. The American Institute AISC specifies the same equation to determine the axial capacity for all composite compressive members irrespective of geometric varieties in steel sections. As supplied by the code, the Eq. (1) is used to determine the design axial capacity of the composite columns under

investigation.

$$P_{AISC} = 0.85A_c f'_c + A_s f_y \quad (1)$$

A_c and A_s are the cross-sectional areas of concrete and stainless steel respectively. The f'_c is denoted as concrete compressive strength in MPa and f_y as the yield strength of stainless steel in MPa taken equal to the 0.2% proof stress. On the other hand, EC4 specifies design regulations for all steel-concrete composite sections with or without reinforcement. The code provides equation to predict design strength for concrete filled tubular columns by taking concrete confinement into account. The specifications in this code is for conventional carbon steel tubes which are assumed to be the same for the stainless steel tubes. The ultimate capacities of concrete filled rectangular and square steel tubes (P_{EC4}) are calculated by the simple summation of the design strengths of concrete and that of the steel comprised (Eq. 2) provided that the ratio of section width to thickness is less than or equal to 52ε where ε = (235/f_y)^{0.5}. The confinement factor, however, is only considered in calculating the capacity of concrete filled circular sections

($P_{EC4\text{ circular}}$) as shown in Eq. (3).

$$P_{EC4} = A_c f_c + A_s f_y \quad (2)$$

$$P_{EC4\text{ circular}} = A_s f_y \eta_2 + [A_c f_c (1 + \eta_1 \frac{t}{D} \frac{f_y}{f_c})] \quad (3)$$

Here, D represents the diameter of the circular steel section and the factors η_1 and η_2 are coefficients of confinement of concrete and steel respectively.

Table 5. Comparison of the strength determined from numerical analysis and design standards.

Group Name	Specimens Designation	Pnum (kN)	PEC4 (kN)	PAISC (kN)	Comparison	
					P_{num}/P_{EC4}	P_{num}/P_{AISC}
G1	S1H	126	138.8	88.8	0.91	1.42
	S1C30	257	331.2	184.07	0.78	1.40
	S1C40	289	286.2	215.3	1.01	1.34
G2	S2H	132	111	88.8	1.19	1.49
	S2C30	254	186.4	180.1	1.36	1.41
	S2C40	287	197.9	210	1.45	1.37
G3	S3H	171	166.6	106.8	1.03	1.60
	S3C30	358	259.6	245.1	1.38	1.46
	S3C40	411	370.1	290.4	1.11	1.42
G4	S4H	121	111.1	106.8	1.09	1.13
	S430	298	177.9	229.1	1.68	1.30
	S4C40	340	191.4	269.1	1.78	1.26
G5	S5H	173	287.9	222.6	0.60	0.78
	S5C30	444	623.8	417.6	0.71	1.06
	S5C40	535	689.7	481.5	0.78	1.11
				Mean	1.12	1.30
				COV	0.31	0.16

5.2 Comparison with Code Predicted Strength

Table 5 represents the comparison between the axial capacity obtained from the current numerical investigation with the design capacity from AISC and EC4 codes as calculated from Eqs. (1), (2) and (3), respectively. For simplification in data representation, the design strengths by EC4 guidelines of circular columns in G5 are denoted as P_{EC4} in the table. It is seen that AISC is more conservative than EC4 predicting the design strength. This might be due to the fact that AISC does not take into account the

effect of confinement of the concrete core by the steel tube²¹. For instance, the design strength predicted by the AISC, P_{AISC} , for group G5 is 6% and 11% less than that predicted by the numerical load Pnum. Also, the Pnum is as high as 42% to 60% as PAISC for column samples in G3. The lesser conservative nature of prediction by EC4 can be observed in the table where the P_{num} is less than PEC4 by 22% to 40% in G5. Reasonable values are obtained when the mean and corresponding COV of P_{num}/P_{EC4} and P_{num}/P_{AISC} respectively, were compared.

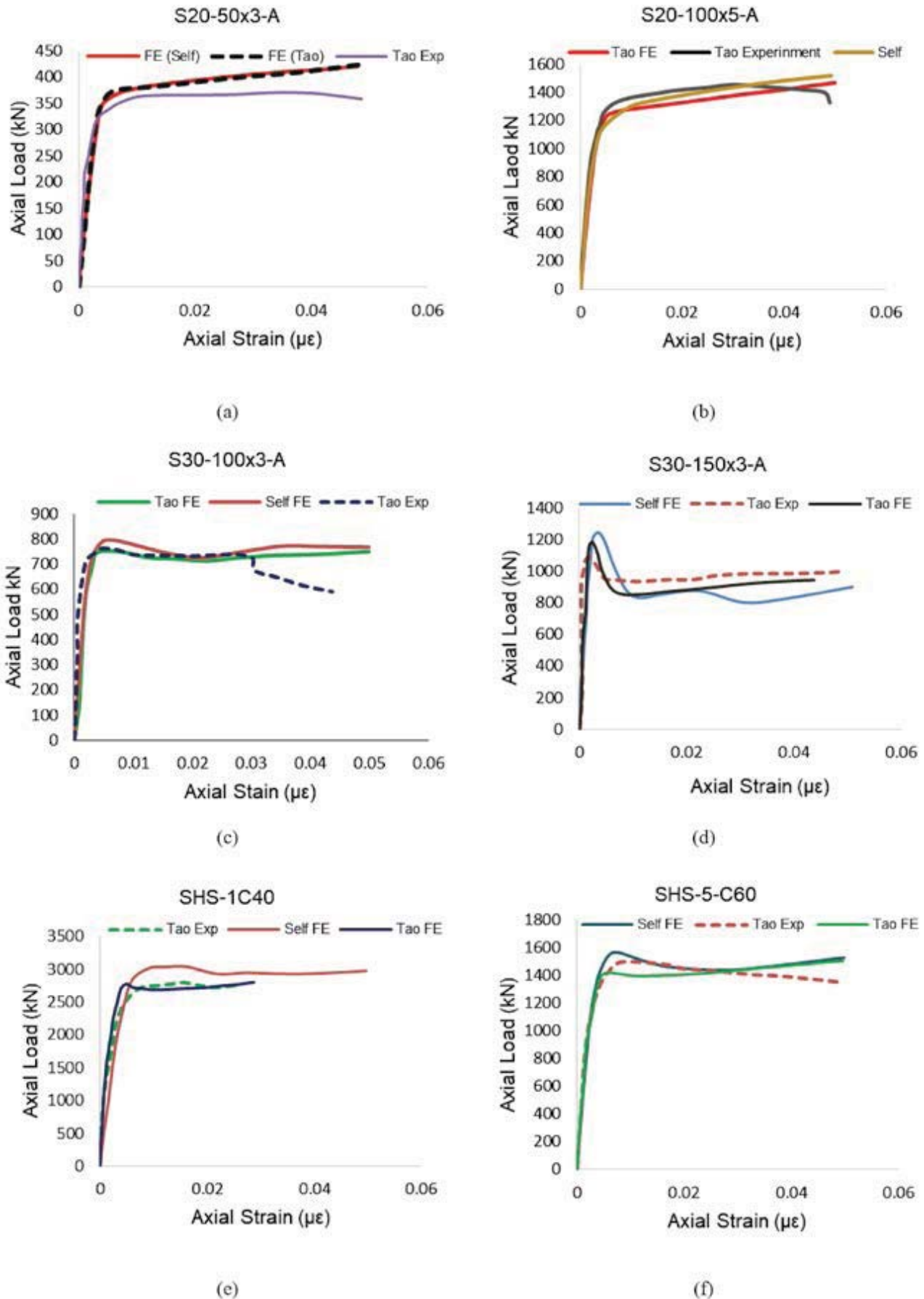


Fig 4. Comparison of the current FE analysis with the published FE analysis and experimental results¹⁶

6.0 CONCLUSIONS

Experimental study was carried out on fifteen CFSST short columns subjected to axial compressive loads. A nonlinear FE analysis was done in order to predict the behavior of the columns in the present study as well as the results published by previous researchers. The following conclusions can be deduced from this study:

- i. The numerical model can predict the behavior and load carrying capacity of CFSST columns under axial compressive loads with very good accuracy.
- ii. Keeping all other factors constant, increasing the strength of concrete from 30 MPa to 40 MPa increased the ultimate capacity of the columns by 15%.
- iii. The existing design codes for CFST columns are conservative in calculating the strength of CFSST columns. This is mainly due to the significant strain hardening of the cold-formed stainless steel tubes compared to its carbon steel counterpart.

7.0 ACKNOWLEDGEMENT

The authors would like to acknowledge STEELTECH for supplying the stainless steel specimens. The expert assistance by the technical staff in the Department of Civil Engineering at Military Institute of Science Technology is also appreciated.

References

- [1] M. S. Rahman, M. Begum and R. Ahsan, Comparison between Experimental and Numerical Studies of Fully Encased Composite Columns, World Academy of Science, Engineering and Technology, International Journal of Structural and Construction Engineering, 10(6), (2016).
- [2] H. Hu, C. Huang, M. Wu and Y. Wu, Nonlinear Analysis of Axially Loaded Concrete-Filled Tube Columns with Confinement Effect. Journal of Structural Engineering, 129(10) pp. 1322-1329, (2003).
- [3] P. Chunhaviriyakul, G.A. MacRae, D. Anderson, C. G. Clifton and R. T. Leon, Suitability of CFT columns for New Zealand Moment Frames. New Zealand Society for Earthquake Engineering, 48(1), (2015).
- [4] Q. Tan, L. Gardner, L. Han and T. Song, Fire performance of steel reinforced concrete-filled stainless steel tubular (CFSST) columns with square cross-sections. Thin-Walled Structures, 143, (2019).
- [5] X.L. Zhao, L.H. Han, H. Lu, Concrete-filled Tubular Members and Connections. CRC Press, London, (2010).
- [6] K. Sakino, H. Nakahara, S. Morino and I. Nishiyama (2010). Behavior of Centrally Loaded Concrete-Filled Steel-Tube Short Columns. Journal of Structural Engineering, 130(2), (2004).
- [7] X.L. Elremali, and A. Azizinamini, (2010). Behavior and strength of circular concrete-filled tube columns. Journal of Constructional Steel Research 58 p. 1567–1591 (2002).
- [8] S.P. Schneider, Axially Loaded Concrete-Filled Steel Tubes. Journal of Structural Engineering, 124(10) pp. 1125-1138, (1998).
- [9] C.S. Huang, Y.K. Yeh, G. Y. Liu, K. C. Tsai, Y. T. Weng, S. H. Wang and M. H. Wu, Axial Load Behavior of Stiffened Concrete-Filled Steel Columns. Journal of Structural Engineering, 128(9) pp. 1222-1230, (2002).
- [10] Z. Tao, B. Uy, L. H. Han and S. H. He. Design of concrete-filled steel tubular members according to the Australian Standard AS 5100 model and calibration. Australian Journal of Structural Engineering 8(3) pp.197–214, (2008).
- [11] A. Roufegarinejad, B. Uy and M. A. Bradford. Behaviour and design of concrete filled steel columns utilizing stainless steel cross sections under combined actions. Australian Conference on the mechanics of Structures and materials, Perth, Australia, p. 159–65, (2004).
- [12] L. Han, C. Xu and Z. Tao. Structural uses of stainless steel — buildings and civil engineering. Journal of Constructional Steel Research, 152, p. 117–131 (2019).
- [13] G. Gedge Performance of concrete filled stainless steel tubular (CFSST) columns and joints: Summary of recent research. Journal of Constructional Steel Research, 64(11), p. 1194–1198 (2008).
- [14] E. Ellobody and B. Young, Design and behaviour of concrete-filled cold-formed stainless steel tube columns. Engineering Structures, 28(5) p. 716–28, (2006).
- [15] E. Ellobody Nonlinear behavior of concrete-filled stainless steel stiffened slender tube columns. Thin-Walled Structures, 45(3) p. 259–73 (2007).
- [16] Z. Tao, B. Uye, F. Liao and L. Han, Nonlinear analysis of concrete-filled square stainless steel stub columns under axial compression. Journal of Constructional Steel Research, 67 pp. 1719–1732, (2011).
- [17] Hibbit, Karlsson and Sorensen, Inc (HKS). ABAQUS/Explicit User's Manual, Version 6.14, (2014).
- [18] Z. Tao, Z. Wang and Q. Yu, Finite element modelling of concrete-filled steel stub columns under axial compression. Journal of Constructional Steel Research, 89 pp. 121–131, (2013).
- [19] AISC, Load and resistance factor design specification for structural Steel buildings. AISC Specification, Chicago (IL USA), American Institute of Steel Construction, (2015).
- [20] Eurocode 4. Design of composite steel and concrete structures, part 1.1, general rules and rules for building. BS EN 1994-1-1: 2004. London (UK): British Standards Institution; (2004).
- [21] E. Ellobody, B. Young and D. Lam, Behaviour of normal and high strength concrete-filled compact steel tube circular stub columns. Journal of Constructional Steel Research, 62(7) pp. 706-715, (2006).